Biometals (2012) 25:875–881
DOI 10.1007/s10534-012-9554-6

XAS analysis of a nanostructured iron polysaccharide produced anaerobically by a strain of *Klebsiella oxytoca*

Iztok Arčon · Oreste Piccolo · Stefano Paganelli · Franco Baldi

Received: 11 September 2011 / Accepted: 26 April 2012 / Published online: 15 May 2012
© Springer Science+Business Media, LLC. 2012

Abstract A strain of *Klebsiella oxytoca,* isolated from acid pyrite-mine drainage, characteristically produces a ferric hydrogel, consisting of branched heptasaccharide repeating units exopolysaccharide (EPS), with metal content of 36 wt%. The high content of iron in the EPS matrix cannot be explained by a simple ferric ion bond to the sugar skeleton. The bio-generated Fe–EPS is investigated by X-ray absorption spectroscopy. Fe K-edge XANES analysis shows that iron is mostly in trivalent form, with a non-negligible amount of Fe^{2+} in the structure. The Fe EXAFS results indicate that iron in the sample is in a mineralized form, prevalently in the form of nano-sized particles of iron oxides/hydroxides, most probably a mixture of different nano-crystalline forms. TEM shows that these nanoparticles are located in the interior of the EPS matrix, as in ferritin. The strain produces Fe–EPS to modulate Fe-ions uptake from the cytoplasm to avoid iron toxicity under anaerobic conditions. This microbial material is potentially applicable as iron regulator.

Keywords Anaerobic growth · Citrate fermentation · Fe–EPS · Fe K-edge · XANES · EXAFS

I. Arčon (✉)
University of Nova Gorica, Vipavska 13, 5000 Nova Gorica, Slovenia
e-mail: iztok.arcon@ung.si
URL: www.ung.si

I. Arčon
Institut Jozef Stefan, Jamova 39, 1000 Ljubljana, Slovenia

O. Piccolo
SCSOP, Via Bornò 5, 23896 Sirtori, Italy
e-mail: orestepiccolo@tin.it

S. Paganelli · F. Baldi
Dipartimento di Scienze Molecolari e Nanosistemi, Università Ca' Foscari Venezia, Calle Larga Santa Marta 2137, 30123 Venice, Italy
e-mail: baldi@unive.it

Introduction

Bio-generated polymeric substances, such as polysaccharides, are able to bind metals, in this way protecting cells from environmental stress. This strategy was also found in a strain of *Klebsiella oxytoca*, BAS-10, isolated from acid drainage mining area enriched with toxic metals (Baldi et al. 2001). The strain can ferment Fe(III)–citrate as the sole energy and organic carbon source to acetic acid and CO_2, producing, during a late stationary phase, a unique exopolysaccharide (EPS), constituted by a branched heptasaccharide repeating unit, which strongly binds Fe(III) (Leone et al. 2007). The binding of Fe in Fe–EPS was studied by cyclic voltammetric measurements, either directly on the hydro-gel or in an aqueous solutions containing Fe(III)–citrate and purified Fe–EPS. From the voltammetric data, the stability formation constant of

Fe(III) with one repeating unit (heptamer) of EPS was found to be about one or two orders of magnitude larger than that of the Fe(III)–citrate complex, and consequently it can be assumed for the Fe(III)–EPS complex a $K \approx 10^{12}$–10^{13} (Baldi et al. 2009). A model was suggested for the iron position in the heptasaccharide unit (Leone et al. 2007), but it could not account for measured Fe concentrations up to 36 wt% (Baldi et al. 2009, 2010). The high content of iron in the EPS matrix cannot be explained by a simple ferric ion bond to the sugar skeleton. The problem deserves a further investigation of the structure of this peculiar iron(III) complex. In this study X-ray absorption spectroscopy methods XANES (X-ray Absorption Near Edge Structure) and EXAFS (Extended X-ray Absorption Fine Structure) are used to obtain structural information about iron in (Fe–EPS) complex at the atomic scale (Ravel and Newville. 2005). With Fe K-edge XANES the valence state of iron in the sample and the local symmetry of its unoccupied orbitals are deduced from the information hidden in the shape and energy shift of the Fe K absorption edge (Wong et al. 1984; Arčon et al. 2007; Küzma et al. 2009; Dominko et al. 2010). In Fe K-edge EXAFS analysis the number and species of neighbor atoms around Fe, their distance from the iron atom and the thermal or structural disorder of their positions are determined (Ravel and Newville. 2005; Küzma et al. 2009; Dominko et al. 2010; Rehr et al. 1992; Coe et al. 1995; Arčon et al. 2005).

Materials and methods

Fe–EPS production and purification

The *K. oxytoca* strain was retrieved from cryovials kept at −80 °C in 25 % glycerol in Nutrient broth (Difco). An aliquot of 1 ml of overnight culture was transferred under anaerobic condition in a medium containing per liter: 2.5 g $NaHCO_3$, 1.5 g NH_4Cl, 0.6 g, 1.5 g $MgSO_4{\cdot}7H_2O$, 1.680 g NaH_2PO_4, 0.1 g KCl, and 50 mM Fe (III)–citrate (13.5 g/l), hereafter referred to as FeC medium, which was buffered at pH 7.6 with NaOH (Baldi et al. 2001). The cultivation of strain BAS-10 was performed in 1 l of FeC medium incubating at 30 °C under anaerobic conditions. After 10 days the suspension was first centrifuged to eliminate bacterial cells, and the supernatant was treated with 800 ml of cooled ethyl alcohol (95 %) to precipitate iron polysaccharide. The purification was repeated twice. The colloidal material was finally dried out under vacuum to obtain Fe–EPS as solid material.

Microscope analysis

During cell growth, several specimens were prepared for transmission electron microscopy (TEM), after hydrogel precipitation. Cells were harvested by centrifugation at 11,000×*g*. The bacterial pellet was fixed for 1 h at 4 °C with 2.5 % glutaraldehyde and 0.1 M lysine in 0.066 M cacodylate buffer, at pH 7.2, for 30 min at room temperature. The cells were washed five times in the same buffer and post-fixed for 1 h at room temperature in 1 % osmium tetroxide, rinsed with distilled water, and embedded in Spurr resin. Ultrathin sections were prepared using a LKB II Nova Ultramicrotome with a diamond knife. Sections were stained with 3.0 % uranyl acetate solution for 15 min, washed once with distilled water and incubated in lead citrate for 10 min. TEM observations were performed with a JEOL JEM 100b (Tokyo, Japan) operating under standard conditions (Baldi et al. 2009). TEM analysis was also used directly without staining preparation. Samples were placed on copper grids to determine Fe–EPS fine structure.

XAFS analysis

Samples of Fe–EPS and of reference iron compounds $FeSO_4{\cdot}7\,H_2O$, Fe_3O_4, α-FeOOH, and Fe_2O_3, with known Fe valence state and structure, were prepared in the form of homogeneous self-standing pellets with the total absorption thickness (μd) of about 1.5 above the investigated Fe K-edge. X-ray absorption spectra of these samples were measured at room temperature in transmission detection mode at the XAFS beamline of the ELETTRA synchrotron radiation facility in Trieste, Italy. A Si (111) double crystal monochromator was used with 0.8 eV resolution at 7 keV. Higher-order harmonics were effectively eliminated by detuning the monochromator crystals to 60 % of the rocking curve maximum. The intensity of the monochromatic X-ray beam was measured by three consecutive ionization detectors respectively filled with the following gas mixtures: 580 mbar N_2 and 1,420 mbar He; 1,000 mbar N_2, 90 mbar Ar and 910 mbar He; 350 mbar Ar, 1,000 mbar N_2 and 650 mbar He. In the XANES region equidistant energy steps of 0.25 eV were used, while for

the EXAFS region equidistant k steps of 0.03 $Å^{-1}$ were adopted with an integration time of 1 s/step. In all experiments the exact energy calibration was established with simultaneous absorption measurement on a 5-μm thick Fe metal foil placed between the second and the third ionization chamber. Absolute energy reproducibility of the measured spectra was ±0.03 eV.

Results and discussion

It was already reported that BAS-10 cells produce Fe(III)–EPS very late in the stationary phase when the medium is spent (Baldi et al. 2001). Cells, observed by TEM, are surrounded by an electrodense EPS structure with iron nano-particles (Fig. 1a). The TEM images of Fe–EPS extract from cells culture show electron dense nanoparticles of different size randomly distributed around the cell. Micrographs of Fe–EPS extracted from cell culture (Fig. 1b) showed amorphous and ordered states of nano-particles as it was previously determined by image analysis (Baldi et al. 2010). In previous reports (Leone et al. 2007; Baldi et al. 2009) it was demonstrated that the strain BAS-10 produces, under anaerobic conditions, a EPS having a branched heptasaccharide repeating unit, the structure of which consists of 4 rhamnose (Rha), 2 glucuronic acids (GlcA) and 1 galactose (Gal) bound by α and β glycosidic bonds:

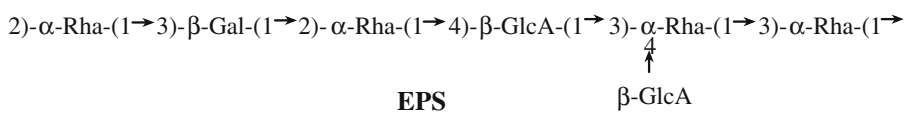

EPS

The EPS structure was confirmed by voltammetric measurements (Leone et al. 2007), FT-IR analysis (Baldi et al. 2010) and NMR.

The Fe K-edge XANES analysis is used in this work to determine the average Fe valence state in the Fe–EPS sample. The analysis of XANES spectra was performed with the IFEFFIT program package ATHENA (Ravel and Newville 2005). The relative K-shell contribution in the absorption spectra (Fig. 2) is obtained by the standard procedure (Ravel and Newville 2005; Wong et al. 1984) by removing the extrapolated best fit linear function determined in the pre-edge region (−150 to 30 eV), and by conventional normalization, extrapolating the post-edge spline background, determined in the range from 100 to 900 eV, to set the Fe K-edge jump to 1.

The energy position of the absorption edge and the pre-edge features are correlated with the valence state of the absorbing atom in the sample. With increasing oxidation state each absorption feature in the XANES spectrum is shifted to higher energies (Wong et al. 1984; Arčon et al. 2007; Küzma et al. 2009; Dominko et al. 2010). For atoms with the nearest neighbors of the same chemical species a linear relation between the edge shift and the valence state has been established (Wong et al. 1984). In our case iron compounds ($FeSO_4 \cdot 7H_2O$, Fe_3O_4, α-FeOOH, and Fe_2O_3) with known Fe valence states between Fe^{2+} and Fe^{3+} and known local symmetry of Fe atom neighborhood were selected for reference. Fe K-edge shift of about 4.5 eV was found between the spectra of the two and three valent iron compounds (Arčon et al. 2007; Küzma et al. 2009; Dominko et al. 2010).

The energy position of the Fe K-edge in Fe–EPS sample is close to the edge position of Fe^{3+} compounds (Fig. 2) confirming that iron in the sample is predominantly ferric ion. The edge shift can be precisely compared only for similar edge profiles. Different environments of the Fe cation, most notably with different site symmetries, result in different K-edge profiles (Arčon et al. 2007; Küzma et al. 2009; Dominko et al. 2010). The precise comparison of the edge shift in such cases is hindered. Among different approaches to determine the average valence state of the atom in the sample from XANES spectra, best results are obtained by a linear combination fit with XANES spectra of proper reference compounds with known valence states of the element, with similar symmetry, same type of neighbor atoms in nearest coordination shells, arranged in a similar local structure.

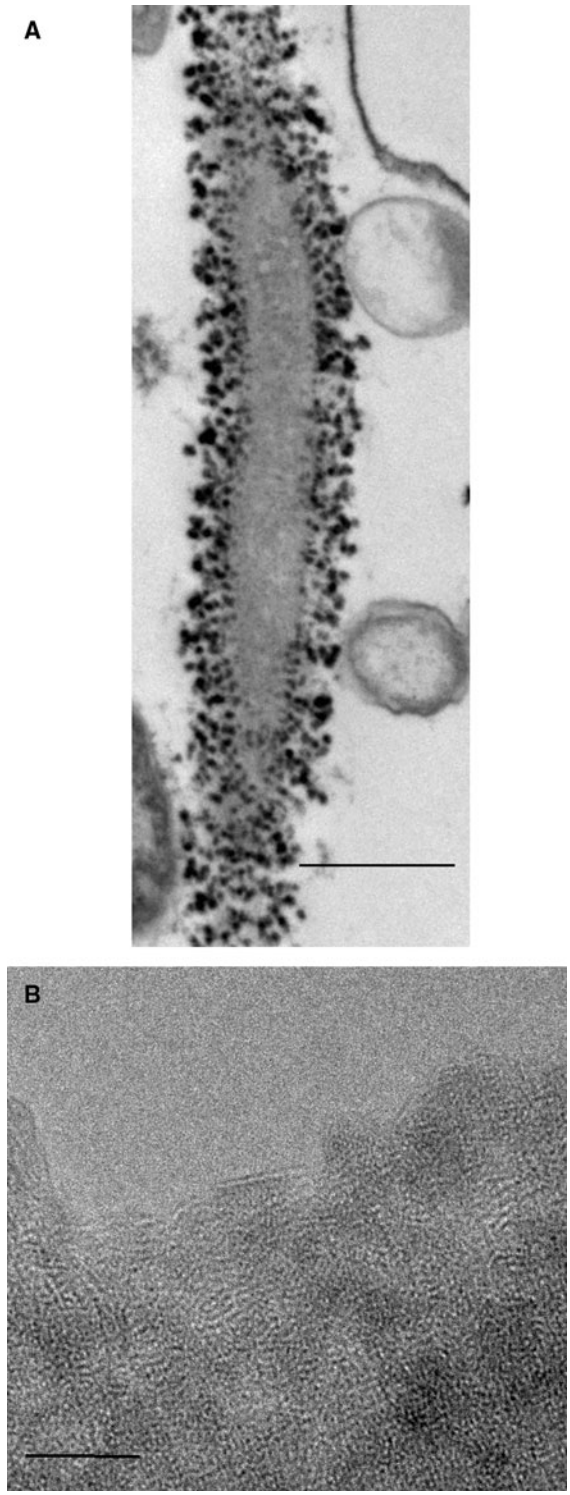

◀ **Fig. 1** **a** TEM micrograph of cell of *K. oxytoca* strain BAS-10 surrounded by electrondense nanoparticles of iron (*bar* 0.5 μm). **b** TEM micrograph of Fe–EPS extracted from bacterial culture with amorphous and ordered states nano-particles (*bar* 50 nm)

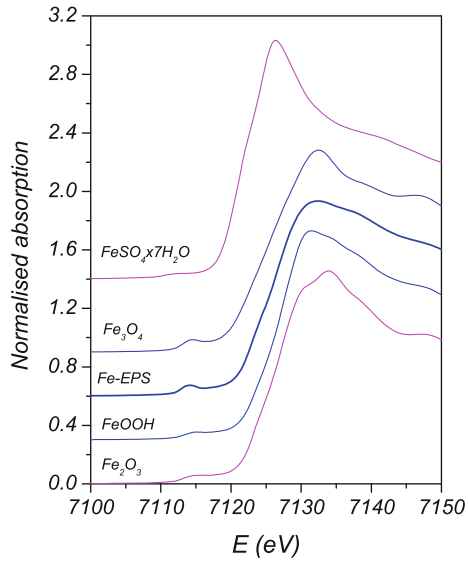

Fig. 2 Fe K-edge XANES spectra of the Fe–EPS sample and reference iron compounds with octahedral iron coordination and different iron valence states between Fe^{2+} and Fe^{3+} ($FeSO_4 \cdot 7 H_2O$, α-FeOOH, Fe_2O_3)

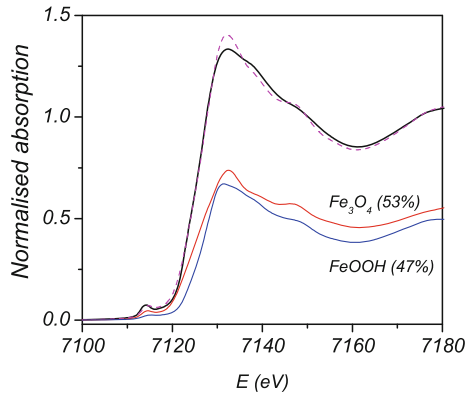

Fig. 3 The Fe K-edge XANES spectrum of the Fe–EPS sample. *Solid line* experiment; *dashed line* best fit linear combination of XANES profiles of Fe_3O_4 (53 %) and α-FeOOH (47 %). Fit components are shown

The Fe XANES spectrum measured on Fe–EPS sample can be very well described by the linear combination of the XANES spectrum of the Fe_3O_4, compound with average Fe valence of 2.67+, and the spectrum α-FeOOH, (pure Fe^{3+}) in the ratio of 53–47 %, respectively. The result of the linear combination fit is illustrated in (Fig. 3). In this way we

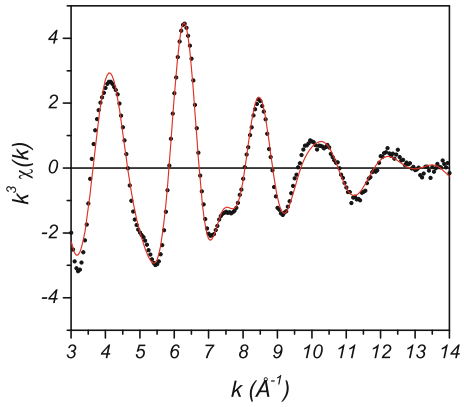

Fig. 4 The k^3-weighted Fe EXAFS spectrum of Fe–EPS sample. Experiment (*dots*); best fit EXAFS model (*solid line*)

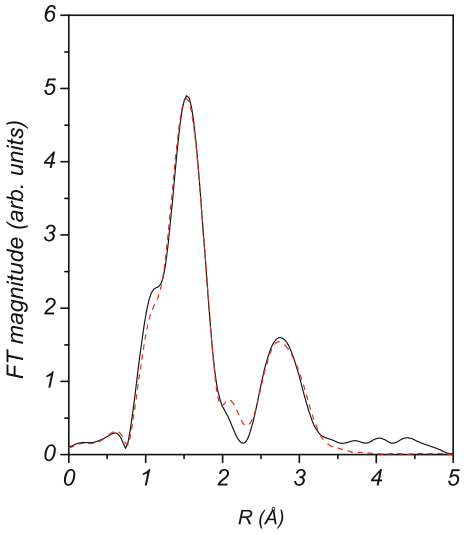

Fig. 5 Fourier transform magnitude of k^3-weighted Fe EXAFS spectra of Fe–EPS sample, calculated in the k range of 3.5–14 $Å^{-1}$. Experiment (*solid line*); best fit EXAFS model (*dashed line*)

determined the average Fe valence in the sample to be 2.82+. The result indicates a presence of mixed Fe valence states, but predominantly Fe^{3+}. About 18 % of iron is in divalent valence state, which could be explained by a presence of nanocrystaline Fe_3O_4 particles with spinel structure.

Fe K-edge EXAFS analysis is used to directly probe the local structure around Fe cations in the Fe–EPS sample. The k^3-weighted EXAFS spectrum of the sample is shown in (Fig. 4). In Fourier transform magnitude of the EXAFS spectrum (Fig. 5) two distinct peaks are observed, representing the

Table 1 Parameters of the nearest coordination shells around Fe atoms in the Fe–EPS sample: average number of neighbor atoms (N), distance (R), and Debye–Waller factor (σ^2)

Fe neigh.	N	R (Å)	σ^2 ($Å^2$)	R-factor
O	5.8(5)	1.97(2)	0.009(1)	
Fe	3.4(6)	3.04(5)	0.018(8)	0.007
Fe	3.2(6)	3.42(5)	0.018(8)	

Uncertainty of the last digit is given in parentheses. A best fit is obtained with the amplitude reduction factor $S_0^2 = 0.72$. The goodness-of-fit parameter, R-factor, is given in the last column

contributions of photoelectron scattering on the nearest shells of neighbors around the Fe atom. A strong peak in the R range between 1 and 2.2 Å can be attributed to photoelectron backscattering on the nearest neighbors around Fe. The second weaker peak in the R range between 2.5 and 3.4 Å represents the contributions from more distant Fe coordination shells.

The quantitative analysis of Fe EXAFS spectrum is performed with the IFEFFIT program package (Ravel and Newville 2005). Structural parameters of the local Fe neighborhood (type and average number of neighbors, the radii and Debye–Waller factor of neighbor shells) were quantitatively resolved from the EXAFS spectrum by comparing the measured EXAFS signal with a model signal, constructed ab initio with the FEFF6 program code (Rehr et al. 1992) from the set of scattering paths of the photoelectron in a tentative spatial distribution of neighbor atoms. The model comprised six oxygen atoms at the same distance in the first coordination shell and iron atoms at two different distances in the second. The atomic species of neighbors are identified in the fit by their specific scattering factor and phase shift.

Three variable parameters for each shell of neighbors are introduced in the model: the shell coordination number (N), the distance (R) and the Debye–Waller factor (σ^2). In addition, a common shift of energy origin ΔEo is also allowed to vary. The amplitude reduction factor S_0^2 is kept fixed at the value of 0.72 in agreement with previous Fe K-edge EXAFS analyses (Dominko et al. 2010). A very good agreement between the model and the experimental spectrum is found using the k range of 3.5–14.0 $Å^{-1}$, and the R range from 1.0 to 3.5 Å (Figs. 4, 5). The list of best fit parameters is given in the Table 1. Six oxygen atoms are identified in the first coordination shell at

the Fe–O distance of 1.97 Å. In the second coordination shell we find six Fe atoms, three at a distance of 3.04 Å and three at 3.42 Å. Relatively large Debye–Waller factors for the Fe coordination shell indicate large disorder in the structure. EXAFS results suggest that iron in the Fe–EPS complex is in a similar form as in ferritin (the iron storage protein) or in polysaccharide iron complex Niferex (Coe et al. 1995; Watt 2011). Iron atoms are coordinated to six oxygen atoms in the first coordination sphere at about the same distance as in ferritin or Niferex. Also the average composition of the second coordination sphere is similar as in ferritin or Niferex. The Fe–Fe distances are the same (within error bars) as in ferritin or Niferex, but the distribution of Fe neighbors at these distances is different (for ferritin and Niferex the authors reported four Fe neighbors 3.06 Å and two Fe at 3.46 Å) (Coe et al. 1995). The comparison of Fe EXFAS spectrum of the Fe–EPS sample with those of bulk crystalline iron oxides or hydroxides (Arčon et al. 2005) clearly shows significant structural differences in the second coordination sphere of the local neighborhood of Fe in the sample. The coordination numbers of iron in the second coordination sphere are significantly smaller than in bulk iron oxides or hydroxides and the distribution of Fe neighbors is different.

EXAFS results thus clearly indicate that iron in the sample is in the mineralized form of iron oxides/hydroxides. The coordination numbers, distribution of neighbor atoms, and large Debye–Waller factor in the second coordination shell show that the structure is not perfectly crystalline like in bulk iron oxides or hydroxides, but rather it is a mixture of different nano-crystalline iron oxides and hydroxides. Taking into account also XANES results which show that iron is predominantly in the form of Fe^{3+}, with a non-negligible amount of Fe^{2+} in the structure, a presence of a spinel structure as in Fe_3O_4 cannot be excluded.

Fe K-edge EXAFS and XANES results prove the presence of Fe oxide–hydroxide cores in Fe–EPS complex, thus explaining the high content of the metal. The result is in agreement with TEM and previous FTIR analysis of Fe–EPS sample, i.e. iron oxide–hydroxides particles are included in the polysaccharide matrix. However, the direct coordination of iron oxide/hydroxides particles to polysaccharide skeleton could not be detected with Fe K-edge EXAFS analysis. The main part of iron atoms is located inside the Fe oxide/hydroxides particles (which are clustering) and only a very small fraction of Fe atoms is on the surface in contact with polysaccharide skeleton. Their contribution to the total Fe EXAFS signal is too small, i.e. below the detection limit.

EXAFS analysis indicates that Fe–EPS structure is very similar (although not identical) to that found for ferritin or for nutraceutical polysaccharide iron complex (Niferex) reported previously (Coe et al. 1995). So Fe–EPS can be functionally related to the class of compounds, which can maintain relatively high concentrations of iron in a soluble, nontoxic form at physiological pH. As such it can be extremely useful in the treatment of anaemia, the illness which can be caused by a deficiency in body iron (Coe et al. 1995). Fe–EPS and/or EPS alone may potentially be applicable as iron regulator.

The Fe–EPS structure has a physiological consistency with the physiology of *K. oxytoca* strain BAS-10, adapted to colonize acid pyrite-mine drainage with elevated concentration of Fe^{2+} and Fe^{3+} in the stream. Iron is a nutrient, but at elevated concentrations becomes toxic, following the dose–effect paradigm. The results show that the strain has developed a mechanism to complex ferric and ferrous ions outside the cell under anaerobic conditions, to cope with large iron level in mine acid stream. During citrate fermentation at late stationary phase the strain secrets this iron molecular complex, where the polysaccharide surrounds a core of iron oxide–hydroxides nanoparticles, to modulate Fe-ions uptake from the cytoplasm, providing in this way iron-resistance. The protective Fe–EPS envelope allows the bacterium to survive for months, without nutrient additions, in spore-like morphological structure (Baldi et al. 2009).

Conclusion

The Fe K-edge EXAFS and XANES structural information on iron in Fe–EPS combined with TEM micrograph of Fe–XEPS show that iron is located in globular nano-particles surrounded by polysaccharide skeleton, explaining the experimental result of high percentage of metal bound to the polysaccharide. Iron in these nanoparticles is in the form of different nano-crystaline iron oxides and hydroxides, predominantly in the form of Fe^{3+}. A non-negligible amount of Fe^{2+} cations indicates a presence of nano-crystalline Fe_3O_4

particles with spinel structure. The presence of oxygen bound to iron is a way for the BAS-10 strain to cope with oxygen stress under anaerobic conditions and to abate iron onto cell surroundings so avoiding iron toxicity, but also taking an advantage of making a hard armor, where cells are preserved for long time under anaerobic conditions. Catalytic applications of Fe–EPS were already presented (Baldi et al. 2010) and possible applications of Fe–EPS as iron supplement or of the chelating agent EPS, depleted by iron, as modulator, under physiological conditions, for people affected by iron overload, are also suggested.

Acknowledgments This research was supported by the Slovenian Research Agency (P1-0112). Access to synchrotron radiation facilities of ELETTRA (beamline XAFS) is acknowledged. Giuliana Aquilanti and Luca Olivi of ELETTRA are acknowledged for expert advice on beamline operation.

References

Arčon I, Mozetič M, Kodre A (2005) XAS study of oxygen-plasma treated micronised iron-oxide pigments. Vacuum 80:178–183

Arčon I, Kolar J, Kodre A, Hanžel D, Strlič M (2007) XANES analysis of Fe valence in iron gall inks. X-Ray Spectrom 36:199–205

Baldi F, Minacci A, Pepi M, Scozzafava A (2001) Gel sequestration of heavy metals by *Klebsiella oxytoca* isolated from iron mat. FEMS Microbiol Ecol 36:169–174

Baldi F, Marchetto D, Battistel D, Daniele S, Faleri C, De Castro C, Lanzetta R (2009) Iron-binding characterization and polysaccharide production by *Klebsiella oxytoca* strain isolated from mine acid drainage. J Appl Microbiol 107:1241–1250

Baldi F, Marchetto D, Zanchettin D, Sartorato E, Paganelli S, Piccolo O (2010) A bio-generated Fe(III)-binding exopolysaccharide used as new catalyst for phenol hydroxylation. Green Chem 12:1405–1409

Coe EM, Bowen LH, Speer JA, Wang Z, Sayers DE, Bereman RD (1995) The recharacterization of a polysaccharide iron complex (Niferex). J Inorg Biochem 58:269–278

Dominko R, Sirisopanaporn C, Masquelier C, Hanzel D, Arčon I, Gaberscek M (2010) On the origin of the electrochemical capacity of $Li_2Fe_{0.8}Mn_{0.2}SiO_4$. J Electrochem Soc 157: A1309–A1316

Küzma M, Dominko R, Hanzel D, Kodre A, Arčon I, Meden A, Gaberscek M (2009) Detailed in situ investigation of the electrochemical processes in Li_2FeTiO_4 cathodes. J Electrochem Soc 156:A809–A816

Leone S, De Castro C, Parrilli M, Baldi F, Lanzetta R (2007) Structure of the iron-binding exopolysaccharide produced anaerobically by the gram-negative bacterium *Klebsiella oxytoca* BAS-10. Eur J Org Chem 31:5183–5189

Ravel B, Newville M (2005) *ATHENA*, *ARTEMIS*, *HEPHAESTUS*: data analysis for X-ray absorption spectroscopy using *IFEFFIT*. J Synchrotron Radiat 12:537–541

Rehr JJ, Albers RC, Zabinsky SI (1992) High-order multiple-scattering calculations of x-ray-absorption fine structure. Phys Rev Lett 69:3397–3400

Watt RK (2011) The many faces of the octahedral ferritin protein. Biometals 24:489–500

Wong J, Lytle FW, Messmer RP, Maylotte DH (1984) *K*-edge absorption spectra of selected vanadium compounds. Phys Rev B 30:5596–5610